PHYSICAL REVIEW B VOLUME 3, NUMBER 2 15 JANUARY 1971

High-Field Saturation of Ultrasonic Attenuation in Copper and Potassium†

W. Royall Cox and J. D. Gavenda
Department of Physics, The University of Texas, Austin, Texas 78712
(Received 31 July 1970)

Ultrasonic attenuation of compressional waves in single-crystal copper and potassium was studied at 4.2 °K in magnetic fields up to 27 kG. Saturation of the attenuation in large fields is found for all directions of $\vec{B}$ in copper with sound propagation along [010] and [$\bar{1}$01]. However, the saturation levels are generally approached as B^{-1}, rather than at the predicted B^{-2} rate, which is found for the case of potassium. The anisotropies of polar plots made by rotating $\vec{B}$ in planes perpendicular to $\vec{q}$ indicate that the high-field attenuation in copper is dominated by orbits running near Brillouin-zone contact regions, rather than by extremal orbits over the main body of the Fermi surface. Tilting $\vec{B}$ out of the high-symmetry crystal planes of copper results in large abrupt decreases in the attenuation at the boundaries of the "dog-bone" and "four-cornered-rosette" hole-orbit regions, which can be attributed to changes in direction (relative to $\vec{q}$) of the open orbits in these regions.

I. INTRODUCTION

Most investigations of the magnetic field dependence of the attenuation of sound waves in pure metals at low temperatures have concentrated on the various resonance effects which occur in relatively weak magnetic fields.[1] These resonances can be attributed to specific bands of electrons on the Fermi surface and are readily interpreted on the basis of idealized models[2] in terms of the corresponding Fermi-surface dimensions. The attenuation in large magnetic fields is also of interest, however, because it depends explicitly on the anisotropies of the electron-phonon interaction (deformation potential) and electron relaxation time. Detailed predictions[3,4] have been made about the behavior of the attenuation in large fields, but no extensive experimental investigation has yet been carried out for any metal. Foremost among the unresolved questions is whether or not open electron orbits can prevent the attenuation from saturating as the magnetic field strength is increased without limit. Similarly, very little is known about the relative contributions from different parts of the Fermi surface to the anisotropies observed in the high-field attenuation for a given experimental geometry.

The attenuation of compressional waves in relatively large transverse magnetic fields has already been studied to a limited extent in several metals. Apparent saturation of the attenuation with increasing field strength was found for a number of metals supporting open orbits as well as for many having closed Fermi surfaces.[1] Attempts to estimate electron relaxation times by fitting high-field data to a B^{-2} law were met with varying degrees of success,[1] but the small ranges of magnetic fields used (usually between 6 and 11 kG) tend to limit the validity of the results. When larger magnetic fields (up to about 20 kG) were used, some evidence[5] of nonsaturation due to open orbits was seen, and the high-field attenuation in ultrapure crystals was found to be extremely anisotropic.

In order to resolve the saturation question and gain some insight into the mechanisms determining the high-field anisotropy, we have carried out a detailed investigation of the compressional-wave attenuation in single-crystal copper and potassium. The experiments were performed at a temperature of 4.2 °K, with sound waves propagating along the [010] and [$\bar{1}$01] crystal axes, and special techniques were employed to ensure precise alignment of the magnetic field.

II. THEORY

The theory of the electronic contribution to the compressional-wave attenuation in strong magnetic fields was first discussed by Kaner,[3] and the anisotropies expected in various geometries were studied in detail by Kaner *et al.*[6] These workers predicted that the high-field attenuation in single crystals with long electron mean free paths l should be very sensitive to the relative orientations of the magnetic field $\vec{B}$, the sound propagation vector $\vec{q}$, and the directions of any open electron orbits. If $\vec{B}$ is tilted out of the plane perpendicular to $\vec{q}$ then the contributions to the attenuation by electrons on both open and closed orbits are generally reduced. Under the conditions $ql \gg 1$ and $\omega\tau < 1$ (where ω is the sound frequency and τ is an average electron relaxation time), the reduction in attenuation with tilt angle ϕ is given approximately by[1]

$$\alpha(\phi)/\alpha(\phi=0) \approx 1/(ql \sin\phi), \quad \sin\phi \gg (ql)^{-1} \ . \quad (1)$$

Similarly, if $\vec{q}$ is rotated by an angle θ in the plane perpendicular to $\vec{B}$ away from a direction perpendicular (in $\vec{r}$ space) to a band of open trajectories, then the attenuation due to the open-orbit electrons falls

off sharply[1]:

$$\alpha(\theta)/\alpha(\theta=0)\approx 1/(ql\ \sin\theta)^2,\quad \sin\theta \gg (ql)^{-1}\ . \quad (2)$$

In both cases, the attenuation decreases are due to the development of a drift velocity along $\vec{q}$, but the magnitude of the effect for a given angular deviation is greater for a rotation of $\vec{q}$ than for a tilt of $\vec{B}$.

From these results, one would expect the anisotropy encountered as $\vec{B}$ is rotated in the plane perpendicular to $\vec{q}$ to be heavily dependent on the locations and orientations of open orbits, with negligible contributions to the high-field attenuation coming from orbits running parallel to $\vec{q}$ in $\vec{r}$ space. Likewise, the theory predicts a general reduction in the attenuation at high fields when $\vec{B}$ is tilted out of the perpendicular plane.

The behavior of the attenuation as the magnetic field is increased without limit has been discussed by Cohen, Harrison, and Harrison[2] for a free-electron gas, and by Pippard,[4] Kaner,[3] and Mertsching[1] for the general case of a real metal. If no open orbits are present, all of these workers predict that the compressional-wave attenuation will saturate when the field becomes strong enough to satisfy the high-field condition, $\omega_c\tau \gg ql$ (where ω_c is the cyclotron frequency). The saturation is expected to proceed as B^{-2}, and the level at which the attenuation saturates in a particular experimental geometry depends upon the sound frequency and the electron mean free paths. If the magnetic field is increased further, to the point where electrical screening[1,2] breaks down, then an inductive[3] absorption becomes important, and the attenuation begins to rise above the saturation level as B^2. However, for high-conductivity metals at low temperatures and moderate frequencies ($f \lesssim 500$ MHz) this breakdown should occur at fields on the order of hundreds of kilogauss and so would not be observable under ordinary experimental conditions.

The effect of open orbits on the compressional-wave attenuation in an increasing magnetic field has not been conclusively resolved by the various theories. Pippard[4] has speculated that open orbits which do not lie along the direction of propagation in $\vec{r}$ space can cause the attenuation of waves propagating perpendicular to $\vec{B}$ to increase indefinitely as B^2 without ever reaching a saturation plateau. According to the calculations of Kaner[3] and Mertsching,[1] however, open orbits cannot prevent the attenuation from saturating, although the saturation levels are highly dependent upon the existence and orientations of such orbits [as indicated in Eq. (2)].

III. EXPERIMENTAL METHODS

A standard pulse-echo technique[7] was used to measure the relative attenuation of compressional waves in magnetic fields up to 27 kG. Most of the data presented here were taken for two single crystals of copper, designated Cu-I and Cu-II, which have residual resistivity ratios ($\rho_{298\,^\circ K}/\rho_{4.2\,^\circ K}$) of 3000 and 35 000,[8] respectively. Some data were also obtained for a single crystal of potassium[9] having a resistivity ratio of about 4000. The copper specimens were oriented to better than 0.5° using the Laue backreflection method, and the faces of all the crystals were spark planed flat and parallel to within 0.0001 in.

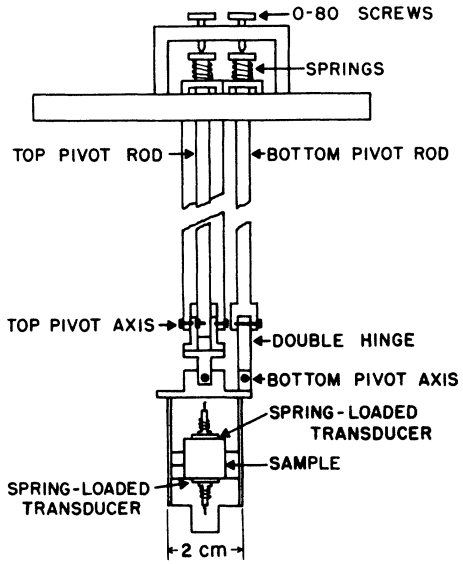

FIG. 1. Schematic drawing of tiltable sample holder.

Because of the great sensitivity of the high-field data to the orientation of $\vec{B}$ relative to $\vec{q}$ and the crystal axes, it proved essential to have some means of accurately orienting the crystals in the plane of rotation of the magnet. This was accomplished by means of the sample holder illustrated in Fig. 1, which enabled the crystals to be tilted about two mutually perpendicular axes in the rotational plane. These two tilt angles, together with the rotation angle in the horizontal plane, provided the three degrees of freedom by which the field could be oriented with an accuracy of better than 0.1°.

The first task in each experimental run was to align the crystal in the Dewar so that the direction of propagation of the ultrasonic wave was perpendicular to the plane of rotation of $\vec{B}$. The procedure involved taking a series of high-field polar plots over a 360° interval at various tilt-angle settings. The magnet turntable was motorized and geared to a potentiometer, so the attenuation could be recorded continously as a function of magnetic field angle in the rotational plane. Two criteria were used to determine when the proper alignment had been achieved. First, a high-field polar plot with $\vec{B} \perp \vec{q}$ should reflect the symmetry of the Fermi

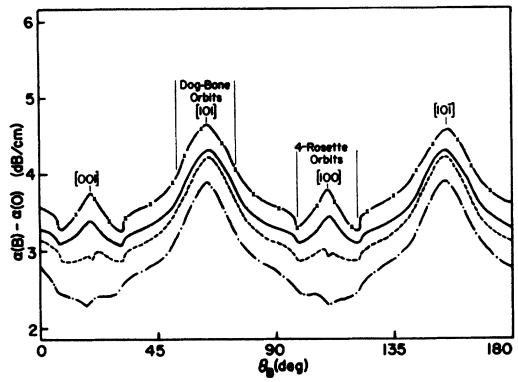

FIG. 2. High-field polar plots for Cu-II with $\vec{B} \perp \vec{q}$, $\vec{q} \parallel [010]$, and $f = 12.0$ MHz. The successive curves are for decreasing values of magnetic field strength, with corresponding f/B values of 0.8 MHz/kG (dash-crossed curve), 1.5 MHz/kG (solid curve), 2.8 MHz/kG (dashed curve), and 4.5 MHz/kG (dot-dashed curve).

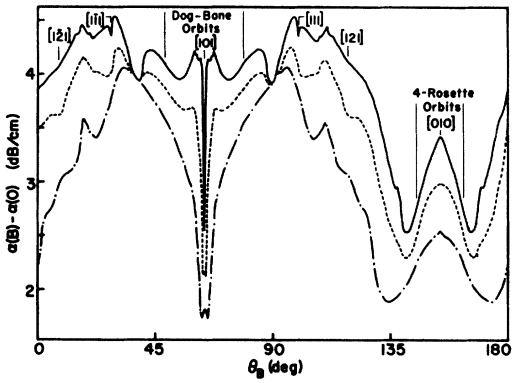

FIG. 4. High-field polar plots for Cu-II with $\vec{B} \perp \vec{q}$, $\vec{q} \parallel [\bar{1}01]$, and $f = 11.8$ MHz. The values of f/B in order of decreasing magnetic field strength are 0.8 MHz/kG (solid curve), 3.5 MHz/kG (dashed curve), and 7.4 MHz/kG (dot-dashed curve).

surface about the propagation direction. Second, the structure of the polar plot should vary in a symmetric way when the crystal is tilted by positive and negative angles of equal magnitude away from the on-axis (aligned) position.

IV. EXPERIMENTAL RESULTS AND INTERPRETATION

A. High-Field Anisotropy

1. *Rotation of* $\vec{B}$ *in the Plane Perpendicular to* $\vec{q}$

The anisotropy of the attenuation in successively stronger magnetic fields can be seen in the polar plots of Figs. 2–4, which were generated by rotating $\vec{B}$ in the plane perpendicular to $\vec{q}$. Since the contribution of a particular electron to the attenuation at high fields depends upon the ratio of cyclotron orbit radius to sound wavelength, one would expect the data to scale with frequency as the field intensity is increased. Accordingly, the ratio of frequency to field intensity is used as a parameter to indicate how far into the high-field ($\omega_c \tau \gg ql$) region the data for each curve were taken. For example, if $f/B \lesssim 5$ MHz/kG, then $r/\lambda \lesssim 0.1$ for single-zone orbits. The various types of orbits encountered for a given direction of magnetic field are indicated in the stereogram of Fig. 5 which was derived from magnetoresistance data.[10]

The data of Figs. 2 and 3, generated by rotating $\vec{B}$ in the (010) plane (along arc AB of Fig. 5),

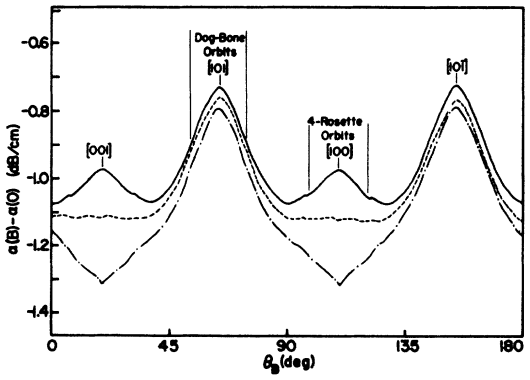

FIG. 3. High-field polar plots for Cu-I with $\vec{B} \perp \vec{q}$, $\vec{q} \parallel [010]$, and $f = 31.8$ MHz. The values of f/B in order of decreasing magnetic field strength are 1.5 MHz/kG (solid curve), 2.9 MHz/kG (dashed curve), and 4.5 MHz/kG (dot-dashed curve).

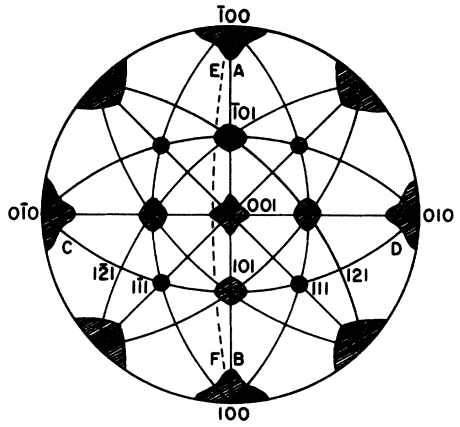

FIG. 5. Sterographic plot of the magnetic field directions giving rise to different types of orbits in copper, determined from magnetoresistance data (after Ref. 10). Periodic open orbits exist for $\vec{B}$ directed anywhere along the great circular arcs, except at the singular points ⟨100⟩ and ⟨111⟩. In the shaded regions there are electron and hole orbits, separated by aperiodic open orbits, but only electron orbits can exist in the clear regions of the stereogram.

reflect the symmetry of the Fermi surface about the [010] axis. The curves for Cu-I are similar to those for Cu-II having the same value of f/B, although the data for the two samples were taken at quite different frequencies and fields. Since the mean free paths of Cu-II exceed those of Cu-I by about a factor of 10, the detailed structure of the Cu-II polar plots is generally sharper than that of the Cu-I plots. However, it was found that this difference in sensitivity can be overcome by increasing the frequency (and field strength) by a factor of 10 for Cu-I to ensure that both crystals have approximately the same value of ql (as well as the same value of f/B). It is seen in Figs. 2 and 3 that with $\vec{q} \parallel [010]$, the attenuation is greatest when the magnetic field is in the [101] (or [10$\bar{1}$]) direction but shows the fastest rise with increasing field strength for $\vec{B}$ along the [100] (or [001]) axis.

The twofold symmetry of the Fermi surface about the [$\bar{1}$01] axis is exhibited in the polar plots of Fig. 4, which correspond to a movement of $\vec{B}$ along arc CD of Fig. 5. It is seen that with $\vec{q} \parallel [\bar{1}01]$ a pronounced dip occurs in the attenuation when $\vec{B}$ is along [101], whereas the absorption here was a maximum in the previous case with $\vec{q} \parallel [010]$. The basis for this difference between the two geometries appears to be the orientation of $\vec{q}$ relative to the open-orbit band directed along [010] in $\vec{k}$ space. In Fig. 4, $\vec{q}$ is parallel instead of perpendicular to the $\vec{r}$-space trajectories of these open-orbit electrons so, by Eq. (2), this band contributes very little to the high-field attenuation. As $\vec{B}$ is rotated away from [101], however, the open orbits coalesce to form extended, closed orbits of rapidly decreasing lengths. The sharp rise in attenuation with field rotation is thought to be due to the increasing contributions made by these orbits as their lengths are reduced and the electrons are able to complete more revolutions before scattering. Likewise, the dip at [101] becomes sharper as the magnetic field intensity is increased and the $\vec{r}$-space lengths of the extended orbits at every field direction near [101] are correspondingly reduced.

A comparison of the general features of the polar plots with the Fermi-surface cross sections[11] encountered as $\vec{B}$ is rotated in the plane perpendicular to $\vec{q}$ leads to some general conclusions about the relative effectiveness of the various orbits in the attenuation process. In general, hole orbits, open orbits perpendicular to $\vec{q}$ in $\vec{r}$ space, and electron orbits running near Brillouin-zone contact regions seem to be better sound attenuators at high fields than electron orbits over the central, "belly" part of the Fermi surface. For example, with $\vec{q} \parallel [010]$ (Figs. 2 and 3) it appears to be the "dog-bone" hole orbits, "lemon" electron orbits, and [010]-directed open orbits which cause the attenuation to increase to a maximum at $\vec{B} \parallel [101]$. The over-all attenuation in the vicinity of [100] is less than that near [101] because none of the electron orbits run near contact regions, but it is the "four-cornered-rosette" hole orbits which begin to contribute at higher fields and produce the local maximum at [100].

The apparently greater contribution to the high-field attenuation from orbits near Brillouin-zone contact regions can be explained on the basis of deformation-potential anisotropy. Pippard has suggested that the deformation potential, and hence the strength of the electron-phonon coupling, may be greatest at the zone boundaries where the electron velocity is small.[12] Indeed, some support for this theory has already come from ultrasonic-attenuation experiments on the noble metals at low fields, where the strongest magnetoacoustic oscillations often arise from orbits running over Brillouin-zone contact points.[13] In the high-field region ($r \ll \lambda$), electrons not on open or extended orbits remain approximately in phase with the sound wave, so the phase-cancellation effects which favor extremal orbits at lower fields may be of lesser importance. Then nonextremal orbits can compete with extremal ones, and one would expect the high-field attenuation to be dominated by those parts of the Fermi surface where the deformation potential is large, i.e., by orbits near contact regions.

The effects of open orbits on the high-field attenuation appear to depend first on their orientations relative to the direction of sound propagation, and second on their complexity and lateral extent in the plane perpendicular to the open direction. This is best illustrated in Fig. 4, where some of the structure of the polar plots seems to be due to the great variation in the degree of convolution of the open orbits encountered as $\vec{B}$ is rotated in the ($\bar{1}$01) plane. For example, when the field is about 15° from [010] these orbits are quite complex in shape and so contribute very little to the attenuation, even though they are perpendicular to $\vec{q}$ in $\vec{r}$ space. As $\vec{B}$ is rotated farther away from [010] the open orbits become less complex, and more closed orbits appear near contact regions, so the general level of the attenuation increases.

2. *Tilt of* $\vec{B}$ *out of the Plane Perpendicular to* $\vec{q}$

A tilt of the plane of rotation of the magnet out of the crystal plane perpendicular to $\vec{q}$ can be achieved by tilting the sample relative to the rotational plane. Then $\vec{B}$ is perpendicular to $\vec{q}$ only along the axis of tilt, so the orbits contributing to the attenuation at every other field angle in the rotational plane may have average velocity components along the propagation direction. Likewise, the field no longer rotates in a symmetry plane of the crystal, but rather in a plane such as that marked EF in the stereogram (Fig. 5); consequently, some of the orbits involved may be fundamentally different in

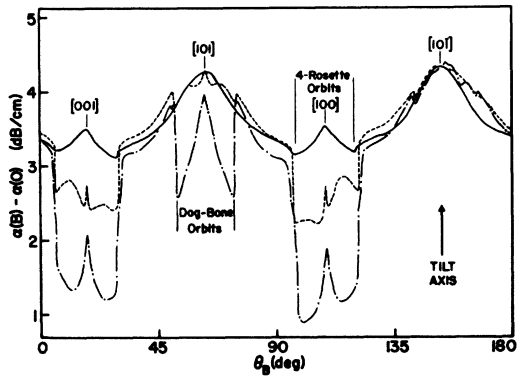

FIG. 6. Polar plots with tilted rotational plane for Cu-II with $\vec{q} \parallel [010]$, $f = 11.4$ MHz, and $f/B = 1.1$ MHz/kG. The angles of tilt $\Delta\theta_T$ out of the (010) plane about the $[10\bar{1}]$ axis are 0° (solid curve), 0.5° (dashed curve), and 1.8° (dot-dashed curve).

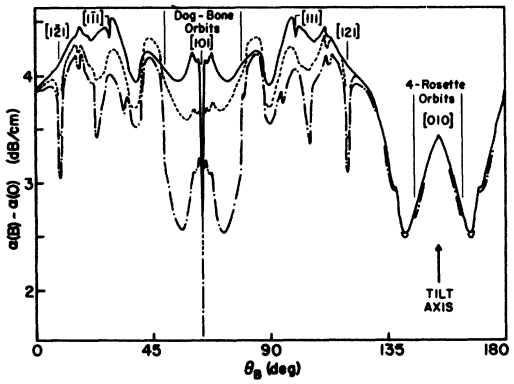

FIG. 8. Polar plots with tilted rotational plane for Cu-II with the same values of $\vec{q}$, f, $\vec{B}$, and $\Delta\vartheta_T$ as in Fig. 7, but with the tilt axis taken along [010].

character (e.g., closed instead of open) from those encountered in polar plots made with $\vec{B} \perp \vec{q}$.

Polar plots made with the rotational plane tilted at various angles out of the crystal symmetry planes are shown for Cu-II in Figs. 6–8. The most striking feature of these "off-axis" plots is the large reductions in attenuation which take place in the vicinity of the dog-bone and four-cornered–rosette hole-orbit regions. The magnitude of the effect increases with tilt angle, and the field directions at which the attenuation drops occur coincide with the boundaries of these regions as determined from magnetoresistance data.[14] Also of interest are the sharp dips in the attenuation which occur at $[12\bar{1}]$ and [121] (Figs. 7 and 8) when $\vec{B}$ is no longer perpendicular to $\vec{q}$. These dips can be attributed to the extended orbits associated with the [111]- and $[1\bar{1}1]$-directed open-orbit bands, respectively, by an argument similar to that already presented for the dip at [101] in the on-axis case.

The magnitudes of the changes in the high-field attenuation which take place when $\vec{B}$ is tilted out of the plane perpendicular to $\vec{q}$ increase with field intensity, as illustrated in Fig. 9. This can also be seen in the off-axis field sweeps of Fig. 10, where the abrupt decrease in attenuation at the four-cornered–rosette hole-orbit boundary becomes more pronounced at the higher fields. Even though the tilt angle is quite small in this case, the magnitude of the drop is great enough to reverse the sign of the slope of the attenuation curve.

An explanation for the sudden decreases in attenuation with magnetic field tilt at the hole-orbit boundaries comes from an examination[11] of the corresponding changes which take place in the orbits there. As long as $\vec{B}$ moves in a symmetry plane of the crystal there are identical periodic open orbits on both sides of the hole-orbit boundaries,

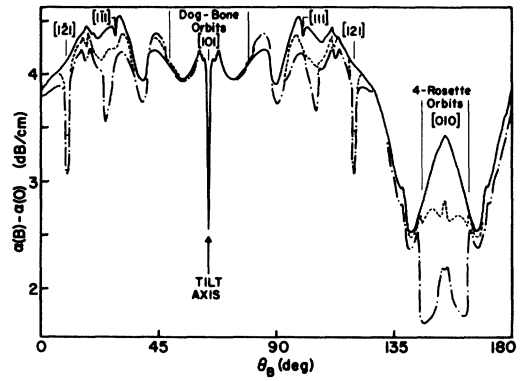

FIG. 7. Polar plots with tilted rotational plane for Cu-II with $\vec{q} \parallel [\bar{1}01]$, $f = 11.8$ MHz, and $f/B = 0.8$ MHz/kG. The angles of tilt $\Delta\theta_T$ out of the $(\bar{1}01)$ plane about the [101] axis are 0° (solid curve), 0.4° (dashed curve), and 1.5° (dot-dashed curve).

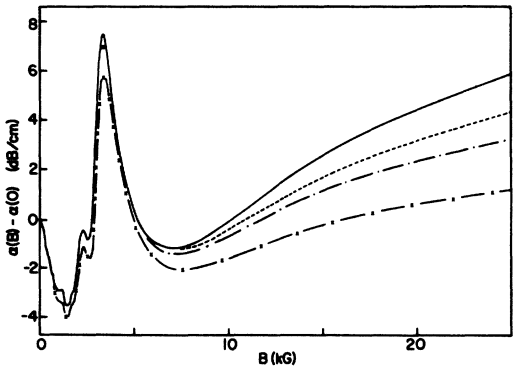

FIG. 9. Magnetic field intensity sweeps for Cu-I with $\vec{q} \parallel [010]$, $f = 91.8$ MHz, and $\vec{B} \parallel [100]$ before tilting. The angular deviations of $\vec{B}$ from the (010) plane are 0° (solid curve), 0.4° (dashed curve), 0.7° (dot-dashed curve), and 1.4° (dash-crossed curve).

which contribute heavily to the attenuation because they are perpendicular to $\vec{q}$ in $\vec{r}$ space. If the plane of rotation of the field is tilted by a small angle out of the symmetry plane [(010) or $(\bar{1}01)$], the open orbits just outside the boundaries coalesce to form extended, closed orbits while those within become aperiodic (or at least lose their short-range periodicity) and are rotated slightly in the plane perpendicular to $\vec{B}$. Since we no longer have $\vec{B} \perp \vec{q}$, both the open and closed orbits develop average velocity components along $\vec{q}$ which cause reductions in the attenuation on both sides of the boundaries in accordance with Eq. (1). However, the change in direction of the open orbits relative to $\vec{q}$ causes an additional loss for these orbits which varies with tilt according to Eq. (2). Thus one would expect the decreases in attenuation with tilt inside the hole-orbit boundaries to be greater than those outside the boundaries by a factor of $(ql \sin\theta)^2$, if all of the attenuation were due to the open orbits. However, the relative attenuation decreases actually observed as the field passes across the boundaries are generally less than $(ql \sin\theta)^2$ because of contributions from other orbits in the hole-orbit regions.

A final point of interest from the off-axis data is the *increase* in attenuation with tilt of $\vec{B}$ out of the plane perpendicular to $\vec{q}$ which takes place with $\vec{q} \parallel [\bar{1}01]$ (Figs. 7 and 8) when $\vec{B}$ is about 20° on either side of [101]. Additional data (not shown) taken at various tilt angles over the range +1.5° to −1.5° confirm that the attenuation in these regions goes through a maximum when $\vec{B}$ and $\vec{q}$ differ from perpendicularity by approximately 0.4°. This behavior is reminiscent of the tilt effect[15] observed in bismuth,[16] but detailed interpretation is difficult in this case, both because $\omega\tau < 1$ and because of the complexities[15] introduced into the theory for a real metal with an open Fermi surface. The small attenuation increases with tilt angle observed in Fig. 6, on the other hand, are thought to be due only to a slight misalignment error (of less than 0.2°) in the on-axis position and so should not be considered as indications of a tilt effect for this geometry.

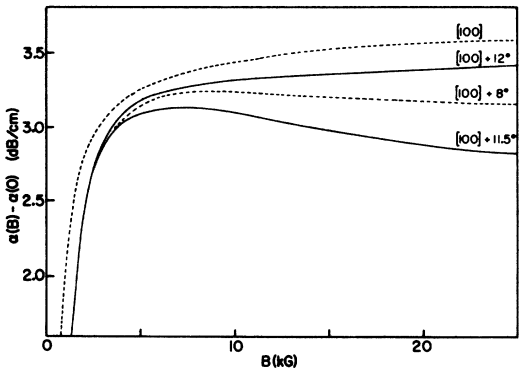

FIG. 10. Magnetic field intensity sweeps for Cu-II with $\vec{q} \parallel [010]$, $f = 12.0$ MHz, and the rotational plane of $\vec{B}$ tilted about 0.2° out of the (010) plane. The various curves correspond to a movement of $\vec{B}$ toward [010] (as in Fig. 6, for example), and the solid lines emphasize the sudden decrease in attenuation as the field passes across the boundary of the four-cornered–rosette hole-orbit region.

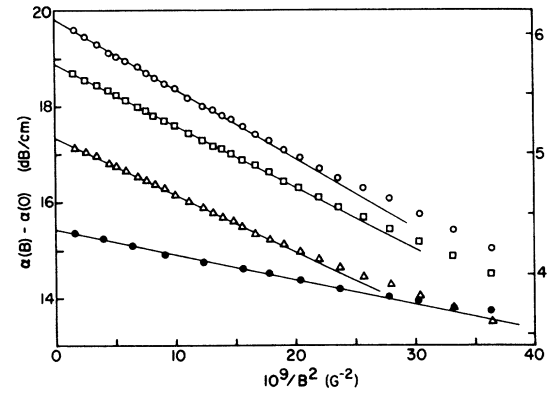

FIG. 11. High-field attenuation values for potassium plotted as a function of B^{-2}. In this case $\vec{q} \parallel [010]$, and data are shown for $f = 51.7$ MHz (left scale) with $\vec{B} \parallel [101]$ (○), $\vec{B} \parallel [100]$ (□), and $\vec{B}$ tilted 2° out of the (010) plane away from [100] (△); and for $f = 30.8$ MHz (right scale) with $\vec{B} \parallel [101]$ (●). Here $r/\lambda \lesssim 0.1$ when $1/B^2 \times 10^9 \lesssim 12$ G^{-2} for the 51.7-MHz data, and when $1/P^2 \times 10^9 \lesssim 34$ G^{-2} for the 30.8-MHz data.

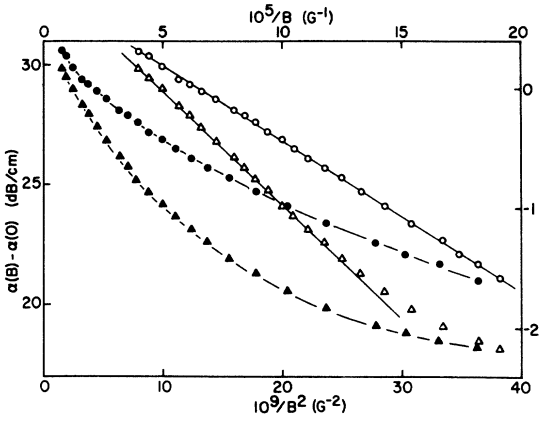

FIG. 12. High-field attenuation values for copper plotted as functions of both B^{-2} and B^{-1}. Data for Cu-II and Cu-I are shown as (○) and (△), respectively, in the B^{-1} plots, and as (●) and (▲), respectively, in the B^{-2} plots. For both samples $\vec{q} \parallel [010]$ and $\vec{B} \parallel [100]$, and the left and right scales are for Cu-II ($f = 33.1$ MHz) and Cu-I ($f = 51.9$ MHz), respectively. Here $r/\lambda \lesssim 0.1$ when $1/B^2 \times 10^3 \lesssim 23$ G^{-2} ($1/B \times 10^5 \lesssim 15$ G^{-1}) for the Cu-II data, and when $1/B^2 \times 10^9 \lesssim 9$ G^{-2} ($1/P \times 10^5 \lesssim 10$ G^{-1}) for the Cu-I data.

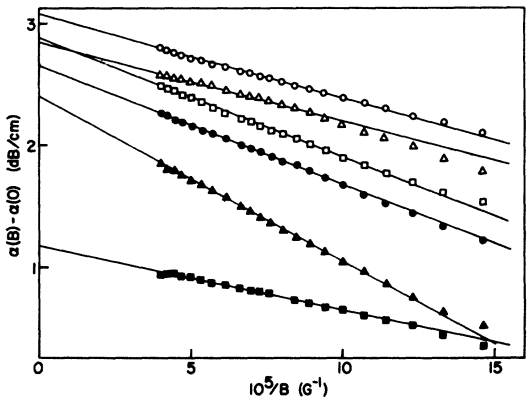

FIG. 13. High-field attenuation values for Cu-I plotted as a function of B^{-1} with $\vec{q} \parallel [\bar{1}01]$, $f = 52.2$ MHz, and with $\vec{B}$ in the following directions in the $(\bar{1}01)$ plane: [111] (O) [101] + 8° (Δ), [121] (□), [010] (●), [010] − 20° (▲), and [101] (■). Here $r/\lambda \lesssim 0.1$ when $1/B \times 10^5 \lesssim 10$ G^{-1}.

B. Limiting Behavior at High Magnetic Fields

Field intensity sweeps like those of Fig. 9 were made for both copper samples at various magnetic field directions and frequencies, and the attenuation was found to approach saturation even in the presence of open orbits. Similar data taken for comparison on a single crystal of potassium indicate a saturation of the attenuation as B^{-2}, in agreement with the theory. It can be seen in Fig. 11 that tilting $\vec{B}$ out of the plane perpendicular to $\vec{q}$ reduces the level at which the attenuation saturates in potassium but does not alter the B^{-2} behavior.

Although the observed universal saturation of the attenuation in copper was expected theoretically,[1,3] the rate at which the saturation levels are approached is somewhat surprising. In Fig. 12 it is seen that with $\vec{q} \parallel [010]$ and $\vec{B} \parallel [100]$ the high-field attenuation in both copper samples saturates more slowly than B^{-2} and, in fact, appears to follow a B^{-1} saturation law. This B^{-1} behavior is found for almost all magnetic field orientations in Cu-I, as illustrated in Fig. 13. The only exceptions are when $\vec{B}$ is near (but not parallel to) [101] or [121], where magnetoacoustic oscillations due to extended orbits show up at high fields, and when $\vec{B}$ is tilted out of the plane perpendicular to $\vec{q}$ near the edge of a hole-orbit region, where the abrupt attenuation decreases (such as in Fig. 10) occur. The data for the larger mean free path Cu-II crystal are much more sensitive to effects such as these and so cannot always be fitted to a constant power law over the entire high-field range. However, when such a fit can be made the Cu-II data also exhibit a B^{-1} dependence, as illustrated in Fig. 12.

No basis for the B^{-1} saturation rate observed in copper can be found in any of the existing theories of ultrasonic attenuation. It can, in fact, be shown[1] that if the relaxation time is independent of the magnetic field (as is usually assumed), then only even powers of B can appear in the high-field attenuation expression. The fact that this anomalous saturation rate is found for many field directions in copper, but does not appear in potassium, points to the possibility that Bragg reflections may be involved. However, no quantitative explanation for this behavior can be offered at this point.

V. CONCLUSIONS

Some general conclusions may be drawn from the anisotropy of the high-field attenuation in copper which may be useful in analyzing similar data for other metals. First, the greatest contribution to the net attenuation at high fields appears to come from orbits running near Brillouin-zone contact regions, rather than from extremal orbits over the central part of the Fermi surface. In particular, the gross features of the polar plots seem to be determined mainly by the open orbits, extended orbits, and lemon-type closed orbits in the vicinity of the [010]-directed open-orbit band; and the next most effective orbits in the attenuation process at high fields appear to be the other periodic open orbits and the hole orbits (e.g., the [111]-directed open orbits and dog-bone-type hole orbits). Second, it may be concluded that the contribution to the high-field attenuation by a particular band of open orbits is extremely sensitive to the direction of sound propagation, since it can vary from a large value to essentially zero, depending upon whether $\vec{q}$ is perpendicular or parallel, respectively, to the open direction in $\vec{r}$ space. Finally, the relative effectiveness of a band of open orbits running perpendicular to $\vec{q}$ in $\vec{r}$ space appears to depend somewhat upon the complexity of the orbit shape, with generally smaller contributions to the high-field attenuation coming from orbits which are extremely convoluted.

Two general conclusions may be drawn from the behavior of the attenuation as a function of magnetic field intensity. First, the attenuation evidently saturates at high fields for any orientation of $\vec{B}$ relative to $\vec{q}$ and the crystal axes. In contrast to the prediction by Pippard,[4] open orbits perpendicular to $\vec{q}$ in $\vec{r}$ space do not appear to be able to prevent saturation, although high-field magnetoacoustic oscillations associated with open orbits running parallel to $\vec{q}$ can sometimes give the appearance of nonsaturation behavior. Second, the attenuation for most field directions in copper appears to satruate as B^{-1}, rather than at the predicted[1,2,4] rate of B^{-2}, which was observed for the case of potassium.

The immediate implications of this study for

future ultrasonic work at high magnetic fields are obvious. First, a resolution of the magnetic field direction to within 0.1° is necessary in order to take accurate high-field data in ultrapure single crystals, and, in the analysis of such data, a B^{-2} saturation rate should not be assumed in advance for metals with open Fermi surfaces. Second, the possibility of drastically different contributions from various parts of Fermi surfaces supporting open orbits should be taken into consideration when trying to extract electron relaxation times from the high-field attenuation.

ACKNOWLEDGMENTS

We wish to express our appreciation to Dr. P. R. Antoniewicz for many helpful discussions and to Dr. L. T. Wood for the use of his computer program based on the model copper Fermi surface developed by Dr. M. R. Halse. We are also grateful to Dr. A. F. Clark for making the high-purity copper available, to Dr. E. Mielczarek for the use of the potassium crystals, and to S. J. Chang and J. P. Masson for their assistance with the experiments.

†Work supported by a grant from the National Science Foundation.

[1]J. Mertsching, Phys. Status Solidi 14, 3 (1966); 37, 465 (1970) and references contained therein.

[2]M. Cohen, M. J. Harrison, and W. A. Harrison, Phys. Rev. 117, 937 (1960).

[3]E. A. Kaner, Zh. Eksperim. i Teor. Fiz. 38, 212 (1960); 39, 1071 (1960) [Soviet Phys. JETP 11, 154 (1960); 12, 747 (1961)].

[4]A. B. Pippard, Proc. Roy. Soc. (London) 257, 165 (1960).

[5]A. R. Mackintosh, Proc. Roy. Soc. (London) A271, 88 (1963).

[6]A. A. Galkin, E. A. Kaner, and A. P. Korolyuk, Zh. Eksperim. i Teor. Fiz. 39, 1517 (1960) [Soviet Phys. JETP 12, 1055 (1961)]; E. A. Kaner, V. G. Peschanskii, and I. A. Privorotskii, *ibid.* 40, 214 (1961) [*ibid.* 13, 147 (1961)].

[7]J. D. Gavenda, in *Progress in Applied Materials Research*, edited by E. G. Stanford, J. H. Fearson, and W. J. McGonnagle (Heywood, London, 1964), Vol. 6, p. 43.

[8]The 35 000 copper was obtained from A. F. Clark, National Bureau of Standards, Boulder, Colo.

[9]Obtained from E. Mielczarek, now at the University of Virginia at Fairfax, Va.

[10]W. A. Reed and E. Fawcett, Science 146, 603 (1964).

[11]See, for example, the empirical model for the copper Fermi surface proposed by M. R. Halse, Phil. Trans. Roy. Soc. London A265, 507 (1969).

[12]A. B. Pippard, in *Documents on Modern Physics*, edited by E. W. Montroll and G. H. Vineyard (Gordon and Breach, New York, 1965).

[13]R. W. Morse, in *The Fermi Surface*, edited by W. A. Harrison and M. B. Webb (Wiley, New York, 1960), p. 214.

[14]A. J. Funes and R. V. Coleman, Phys. Rev. 131, 2084 (1963).

[15]H. N. Spector, Phys. Rev. 120, 1261 (1960).

[16]D. H. Reneker, Phys. Rev. 115, 303 (1959).

PHYSICAL REVIEW B VOLUME 3, NUMBER 2 15 JANUARY 1971

Displaced Distribution Functions for Three-Phonon Umklapp Processes

Y. P. Joshi*
Physics Department, Allahabad, University, Allahabad, India

and

G. S. Verma
Physics Department, Banaras Hindu University, Varanasi, India

(Received 12 November 1969)

It is shown that three-phonon umklapp processes tend to displaced Planck distributions that are characterized by the reciprocal-lattice vectors of the crystal.

Since the phonon frequency and the phonon group velocity are periodic functions of the phonon wave vector, it is a convenient representation to describe the wave vector in the reduced-zone scheme. The distinction between the three-phonon normal and umklapp processes occurs only in this scheme. It is well known that in the presence of an equilibrium thermal gradient, the normal processes tend to a displaced Planck distribution. [1–4] This is because these processes conserve the phonon wave vector (or phonon monemtum), and the distribution to which they tend should be consistent with this condition. We put some arguments in the following to emphasize that similar distribution functions also exist for the three-phonon umklapp processes.

If a phonon is represented by $(\vec{q}j)$, where $\vec{q}$ is the phonon wave vector and j the polarization index, then the three-phonon processes are described by